

One of the most promising structural materials in gas turbine engineering is the alloys based on an intermetallide, the type of Ni_3Al , with an equiaxial and directional columnar structure. These materials make it possible to increase the working temperature of blades to 1,220 °C. The blades are made by the method of precise casting in a vacuum; in this case, it is necessary to technologically join the nozzle blades into blocks, to fix the signal holes in cooled blades, to correct casting defects.

Welding by melting intermetallide materials, as well as other cast heat-resistant nickel alloys (HNA), does not yield positive results. Therefore, various brazing techniques are used such as TLP-Bonding (Transient Liquid Phase Bonding). Filler metals' melting point is lower than that of the main metal. The key issue related to the technology of brazing HNA, including the design of appropriate filler metals, is the improvement of the physical-mechanical and operational properties of brazed joints.

This paper reports the established rational doping of a filler metal base, as well as depressants, the critical temperatures and surface properties of filler metals, their chemical composition, the structure and properties of brazed joints, the mode parameters, and brazing technology. To improve the stability of the structure and the high-temperature strength of the brazed joints, the filler metal was alloyed with rhenium and tantalum. Mechanical tests of brazed joints at 900 °C were conducted in Ukraine; at a temperature of 1,100 °C – in the People's Republic of China. The test results showed that the short-term strength of alloy compounds with an equiaxial structure based on the Ni_3Al -type intermetallide at 1,100 °C is 0.98 of the strength of the main metal. The long-lasting strength at the same temperature meets the requirements for the strength of the main metal

Keywords: brazed joints, microstructure of joints, chemical composition, short-term and long-lasting strength, brazing technology, tantalum, rhenium, boron

UDC 621.791.3

DOI: 10.15587/1729-4061.2020.217819

DESIGNING BRAZING FILLER METAL FOR HEAT-RESISTANT ALLOYS BASED ON Ni_3Al INTERMETALLIDE

V. Kvasnytskyi

Doctor of Technical Sciences, Professor
Department of Welding Production
National Technical University of Ukraine
«Igor Sikorsky Kyiv Polytechnic Institute»
Peremohy ave., 37, Kyiv, Ukraine, 03056
E-mail: kvas69@ukr.net

V. Korzhyk

Doctor of Technical Sciences, Senior Researcher, Director*

V. Kvasnytskyi

Doctor of Technical Sciences, Professor**

H. Mialnitsa

PhD, Associate Professor, Deputy Head of Metallurgy Department
Gas Turbine Research And Production Complex Zorya-Mashproekt
Bohoiavlenskyi ave., 42a, Mykolaiv, Ukraine, 54018

Chunlin Dong

Doctor of Engineering, Professor, General Director*

T. Pryadko

PhD, Head of the Laboratory
Laboratory of Eutectic Alloys

G. V. Kurdyumov Institute for Metal Physics
of the National Academy of Sciences of Ukraine
Akademika Vernadskoho blvd., 36, Kyiv, Ukraine, 03142

M. Matviienko

PhD, Associate Professor
Department of Welding
Kherson Branch Admiral Makarov National University of Shipbuilding
Ushakova ave., 44, Kherson, Ukraine, 73003

Y. Buturlia

Postgraduate Student**

*Guangdong Welding Institute

(E.O. Paton Chinese-Ukrainian Institute of Welding)
Changxing Road, 363, Tianhe, Guangzhou, China, 510650

**Department of Welding Production

Admiral Makarov National University of Shipbuilding
Heroiv Ukrainy ave., 9, Mykolaiv, Ukraine, 54025

Received date 22.10.2020

Accepted date 25.11.2020

Published date 22.12.2020

Copyright © 2020, V. Kvasnytskyi, V. Korzhyk, V. Kvasnytskyi,

H. Mialnitsa, Chunlin Dong, T. Pryadko, M. Matviienko, Y. Buturlia

This is an open access article under the CC BY license (<http://creativecommons.org/licenses/by/4.0>)

1. Introduction

Heat-resistant nickel alloys (HNA) are the main structural material in gas turbine engineering. The efficiency

of gas turbines depends significantly on the temperature of the gas before the turbine. Therefore, the working temperature of HNA continuously increases. From 1970 to 2000, the efficiency of engines of different generations in-

creased. The maximum gas temperature at the inlet to the turbine increased from 1,027–1,177 °C (third generation) to 1,527–1,677 °C (fifth generation) [1, 2]. The most thermally loaded are the nozzle and working blades made by the method of precise casting in a vacuum. To reduce the temperature, the blades have a complex cooling system; to increase heat resistance, they are made in a monocrystalline fashion or with directed crystallization. New alloys with more complex doping have been designed, involving the use of computer calculations, for example, PHACOMP, the software package for computing the physical-chemical and mechanical properties of alloys, JMatPro, the software suite for simulating the properties of alloys, and others. Scientists considered the possibility of creating both the targeted crystallized compositional materials and alloys with a polycrystalline structure based on the intermetallide Ni₃Al, whose working temperatures could be raised to 1,220 °C [2, 3]. Intermetallide alloys are the most promising for the next-generation aircraft gas turbines.

2. Literature review and problem statement

The Ni₃Al intermetallide-based alloys are used in China (89JG 4010 (IC10)), Russia (VKNA type), the United States, and other countries [4, 5]. The mechanical and operational properties of some alloys are described in works [6, 7].

The widespread use of new materials to create high-performance gas turbines is largely determined by the ability to join these materials. For example, it is required to combine nozzle blades into blocks, to patch holes in the cast blanks of cooled blades. The holes designed to fix a ceramic rod in the ceramic mold should be brazed. Surface casting defects and operational defects of blades must also be corrected. The difficulties of welding by HNA melting are associated with the low resistance of joints against crystallization and subsolidus cracks, cracking during thermal treatment, as well as ensuring their heat resistance and thermal stability. These issues are predetermined by the melting and overheating of the main metal, as well as the reduction of plasticity in the temperature interval of fragility to zero [8–10]. When melting alloys made by the directional crystallization, they lose their original structure. Therefore, modern high-temperature casting alloys are almost not welded by melting.

More promising are techniques of welding in a solid state, such as diffusion welding with intermediate layers, including melting [11], friction welding [12], as well as brazing [13]. Brazing is the most universal process that is widely used in gas turbine engineering. It helps avoid the overheating of alloys but has certain limitations.

The main issue related to the technologies of brazing the new generation of heat-resistant alloys, including the design of appropriate filler metals, is the improvement of the physical-mechanical and operational properties of brazed joints, close to the properties of the main metal. The relevance of advancements increases when brazing the new generation materials based on the Ni₃Al intermetallide, which have a high melting temperature and demonstrate thermal stability of the structure up to the melting point.

Diffusion welding and brazing, brazing under pressure, brazing with a compositional filler metal, etc. are used to resolve this issue [14]. The international literature adopted the term TLP-connection (Transient Liquid Phase Bonding) [4, 15, 16]. The term first appeared in the “Welding

Journal” in the late 1950s. In diffusion welding with a melting intermediate layer, the liquid phase is pushed out of the joint. Its remnants in the form of a very thin layer (up to a few μm) are dissolved, due to linear diffusion, perpendicular to the joint. In the TLP-joint, there is the isothermal crystallization of a filler metal due to the volumetric processes of dissolution of the main metal and diffusion. At the same time, the temperature of the brazing, the size of the clearance, and the time of brazing play a big role. The choice of alloying elements, depressant elements, as well as their interaction with the main metal, are important.

Currently, there are many filler metals for high-temperature applications. However, each brazed material requires an individual approach when choosing the composition of filler metal, due to its structural features, specific operating conditions, and the required mechanical properties of brazed joints. Therefore, much attention is paid to the research that determines the choice of the chemical composition of the filler metal and the parameters of the technological regime of brazing. The use of filler metals, similar in chemical composition to the brazed material, owing to the phase transformations, occurring under unbalanced conditions during brazing and subsequent heat treatment, makes it possible to obtain the structure of a brazed seam, close to the microstructure of the main metal.

Filler metals for HNA are designed on the basis of nickel, which is doped with elements that provide for the thermal stability and heat-resistance of the alloy. To reduce the melting temperature of the alloy and filler metal, the depressants are added [16, 17]. Paper [4] reports the results of studying the brazed joints of the alloy IC10 using the filler metal BH2. The filler metal contains (% by weight) 2.4 B and 2.6 Hf, which is also included in the alloy IC10 (1.0–2.0 % by weight). A state diagram of the Hf-Ni system is given in work [17]. The concentration of other elements was (5.4–5.5) Al; (7.1–7.3) Cr; (12.1–12.3) Co; (1.5–1.6) Mo; (6.7–6.9) Ta; (4.9–5.2) W; to 0.1 C; Ni is the rest. The brazing was performed at a temperature of 1,250–1,270 °C in a high-vacuum furnace. The time required for the isothermal seam hardening is 2.66, 3.55, and 4.72 hours at temperatures of 1,250, 1,260, and 1,270 °C, respectively, that is, increasing the temperature of brazing increases the time [4]. The mechanical properties of the brazed joints were not investigated in the cited work but, given the seam structure, the high concentration of boron in the filler metal, and the presence of eutectics, they would not be high.

To braze the alloy VKNA-4U based on Ni₃Al with the alloy EP975, the authors of works [18, 19] used the complex alloyed filler metals VPr24, VPr27, VPr47, VPr48, VPr36, to connect the disc to the blades. All filler metals demonstrated good wetting and filling of clearances but, except for the filler metal VPr36, they formed solid eutectic layers, dramatically reducing the strength of joints at working temperatures. At the same time, the chosen joint does not make it possible to compare its strength with the strength of the main metal.

In paper [20], in order to increase the strength of the brazed joints of the alloy VZhL12U, the authors used a boron-containing filler metal with a silicon additive. The mechanical properties of such joints involving the alloy ZhS26VY are described in [21]. To increase the strength of joints involving the alloy ZhS6U, the authors of [22] used a VPr36-based composite filler metal; a mixture of the filler metal VPr36 and the silicon-containing filler metal NS-12

was used in works [23, 24]. The use of silicon-containing filler metals is not logical for a Ni₃Al-based alloy as in these alloys a silicon content is strictly limited (to 0.2 %).

Studies [25, 26] investigated the filler metals VPr37 and VPr44 for brazing the heat-resistant alloys ZhS36 and ZhS32. These filler metals, as well as the filler metal VPr36, were recommended by the All-Russian Institute of Aviation Materials (VIAM) for brazing heat-resistant alloys based on the Ni₃Al intermetallide.

Papers [27, 28] reported studies into the multicomponent filler metals of the Ni-Cr-Ti-Nb-Al-(Me)-Zr system. The results helped select two filler metals containing 2.0 and 1.0 % of Zr. The temperature of the liquidus and solidus is 1,231 and 1,101 °C, respectively, for the filler metal with 2.0 % of Zr, and 1,259 and 1,141 °C – for the filler metal with 1.0 % of Zr. Using the received filler metals, the authors brazed the samples made from the alloy ZhS6U at the liquidus temperature of each filler metal over 5 minutes, followed by thermal treatment at 1,220 °C over 4 hours. The durability of the samples was determined at the joints of flat samples at 975 °C and under a stress of 140 MPa. The destruction of the brazed samples occurred within 18...19 hours with the filler metal containing 2.0 % of Zr, and 41...60 hours with the filler metal containing 1.0 % of Zr, which is much lower than that of the main metal.

All this allows us to suggest that it is appropriate to conduct a study aiming at improving the long-lasting strength of a brazed joint.

3. The aim and objectives of the study

The aim of this study is to design a filler metal and a brazing technology for the alloy IC10 based on the Ni₃Al intermetallide, which would ensure the short-term and long-lasting strength at stretching of the cylindrical joint samples with an interlayer thickness of 0.08 mm not less than 80 % of the strength of the main metal, at a test temperature of 1,100 °C lasting over 100 hours.

To accomplish the aim, the following tasks have been set:

- to determine the rational alloying of the filler metal base relative to the IC10 alloy;
- to choose a depressant for the filler metal;
- to investigate the surface properties of filler metals and their interaction with the IC10 alloy;
- to investigate the structure, chemical composition, and properties of brazed joints;
- to devise the IC10 alloy brazing technology.

4. The materials, equipment, and research methods to study the structure, composition, and properties of the filler metal and brazed joints

The filler metal design was based on the obvious axiom. If one strives to make a brazing joint, close to the main metal by mechanical properties, it is necessary that the joint composition should be close to the composition of the main metal. The brazing process implies that the filler metal temperature should be lower than the melting point of the main metal. To this end, depressants are introduced into the filler metal. Therefore, the first stage involves the selection of the filler metal base close in its composition to the main metal; it is additionally supplemented with more efficient hardeners. That employs computer software for the calculation of heat-resistant alloys. In the second

stage, the depressant and its amount are chosen based on the results from experimental studies of interaction between the base of the filler metal and a heat-resistant alloy.

We used the alloy based on Ni₃Al 89IG4010 (IC10) manufactured in the People's Republic of China, designed to produce nozzle blades with directional crystallization for aircraft gas turbines. The alloy contains (% by weight): (0.07–0.12) C; (6.5–7.5) Cr; (11.5–12.5) Co; (4.7–5.2) W; (1.0–2.0) Mo; (5.6–6.2) Al; (6.5–7.5) Ta; (1.0–2.0) Hf; Ni is the rest. There are also (0.01–0.02) B in the alloy; to 0.1 Zr; to 0.2 Si; to 0.2 Mn; to 0.01 S; to 0.015 P. Cylindrical samples with a diameter of 20 mm and a height of 40 mm were used for research, which were exposed to a full standard thermal treatment. The main metal was melted in an induction vacuum furnace. It was used to cast the samples into a mold at 1,480–1,550 °C in a vacuum furnace with directional crystallization at an extraction rate of 2.5 to 7.0 mm/min.

Due to the limited number of samples supplied by the customer, the IC10 alloy analog was smelted. The concentration of alloying elements in the analog was within the interval of the rated concentrations of the IC10 alloy. At the same time, one of the analogs was additionally doped with titanium. The comparative chemical composition of the IC10 alloy, smelted in China, as well as its analogs, is given in Table 1.

Table 1
Concentration of elements in the IC10 alloy and its M1 and M2 analogs

Alloy type	Chemical composition, % by weight									
	C	Cr	Co	W	Mo	Al	Ta	Hf	Ti	Ni
IC10	0.09	7.0	12.0	5.0	1.5	5.9	7.3	1.4	–	bas.
Analog (M1)	0.06	7.19	11.83	5.10	1.67	5.74	6.86	1.46	2.0	bas.
Analog (M2)	0.085	6.6	11.63	4.67	1.40	5.61	7.44	1.6	–	bas.

The standard thermal treatment of the IC10 alloy involves homogenization with heating up to 1,180 °C with a 2-hours aging, followed by heating to 1,265 °C with a 2-hour aging and cooling in the air, then heating up to 1,050 °C with a 4-hour aging and cooling in the air.

The 80-g experimental filler metals were smelted in a laboratory electric arc furnace with a non-consumable tungsten electrode on a cooled copper pod by six-fold melt in the environment of purified argon containing 0.003 % O₂, 0.03 g/m³ H₂O.

The brazing of cylindrical samples was performed at the installation UDSV-DT in a vacuum of 10⁻² Pa, at the ultrahigh vacuum manufacturing complex VVU-1D (a vacuum of 10⁻⁴ Pa), and in the vacuum furnace SNV-1.3.1/20I1 (a vacuum of 5·10⁻³ Pa). The VVU-1D installation is equipped with a gas launch system to control the composition of the residual atmosphere using two mass-spectrometers MH7304, upgraded by the manufacturer. The installation uses high-frequency current heating with a capacity of 100 kW. The oil-free vacuum 10⁻⁴ Pa is created by an electric arc vacuum pump.

Structural studies were carried out using optical metallography and raster electron microscopy, as well as X-ray structural analysis.

Light microscopy was performed at the microscopes Neofote-21 (Germany) and Versamet-2 (USA). The structure of alloys was defined by chemical etching in a solution consisting of 10 grams of chlorine iron, 30 ml of hydrochloric acid, and

120 ml of alcohol. To differentiate carbides and a sigma phase, we used a reactive by Murakami: 10 grams of red blood salt, 10 grams of caustic potassium, or 7 grams of caustic sodium.

Raster electron microscopy and a local X-ray spectrometer microanalysis were carried out at REMMA 102-02 (Ukraine) and JSM-840 (Japan) installations equipped with wave and energy-dispersion spectrometers.

X-ray structure analysis was carried out at the DRON-4M1 diffractometer (Russia).

Differential thermal analysis was carried out at the VD-TA-8M thermoanalyzer (Ukraine). The heating and cooling rates were automatically maintained at 0.8 °C/s. The samples weighing one gram were placed in the crucibles made from Y₂O₃ yttrium oxide. High-purity helium was used to protect the samples.

The short-term and long-lasting strength of the brazed samples at 1,100 °C was determined in China (China Electronic Product Reliability and Environmental Testing Research Institute (CEPREI) at the GWT-2105 installation.

5. Results of studying the structure, composition, and properties of the filler metal and brazed joints

5.1. Determining the rational alloying of the filler metal base relative to the IC10 alloy

According to electron microscopy, the structure of the directed crystallized alloy IC10 (a slice across the axis) and its polycrystalline analog M2, as well as their chemical composition (Fig. 1), are identical.

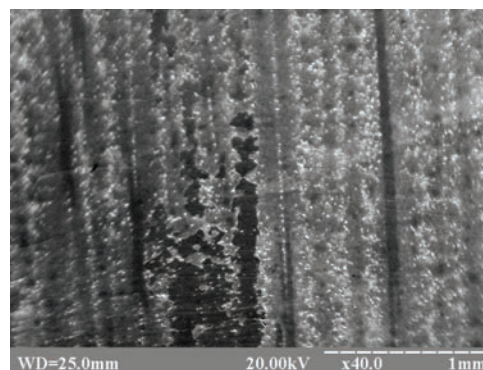
Our analysis of the differential thermal curves for the alloy IC-10 produced in the PRC (Fig. 2, *a*) and its analog M2 (Fig. 2, *b*) established that the temperatures of phase transformations during melting and crystallization coincide within the margin of a measurement error.

The comparative studies of wetting and interaction involving the experimental filler metals and the alloy IC10 and its analog produced almost identical results. Therefore, preliminary studies were conducted on the analog to IC10 (M2). The M1 analog was smelted to estimate the titanium distribution by phase.

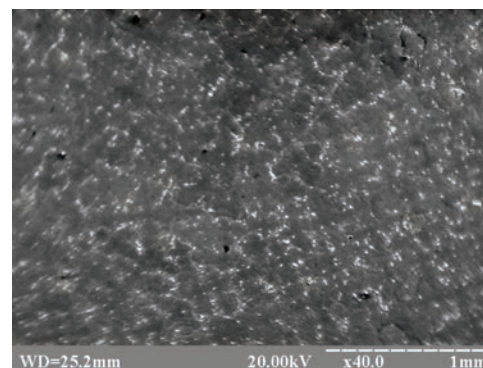
The task of determining the rational alloying of the filler metal base is related to the chemical composition of the IC10 alloy. It was assumed that, in order to make joints with the properties close to the properties of the main metal, their compositions must also be close, taking into consideration the alloy features. However, the IC10 alloy lacks the most effective element in terms of increasing a hardening capacity – rhenium [1–3, 29–31].

Rhenium, which has the maximum elasticity module ($E_{Re}=463$ GPa, $E_w=411$ GPa, $E_{Mo}=329$ GPa, $E_{Ta}=186$ GPa), is responsible for the greatest contribution to the consolidation of solid solution [29]. It increases the solubility of the interstitial additives; under its influence, most of tungsten enters the intermetallide γ -phase [30]. Alloying by rhenium reduces the diffusion mobility of atoms characterized by the nickel self-diffusion factor, which increases the long-lasting strength of alloys [31].

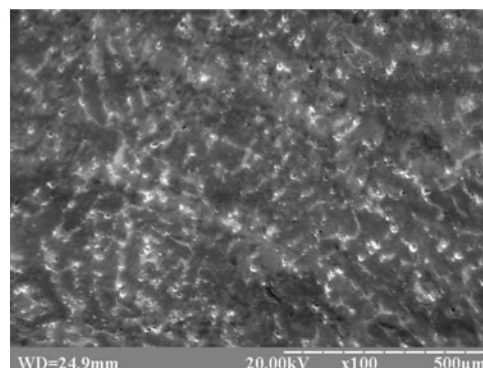
However, the alloying of the filler metal base by rhenium, in addition to increasing the stability of the structure and the high-temperature strength of the brazed joints, leads to an increase in the melting temperature, and the number of electronic vacancies in the alloy, which determine the risk of alloy embrittlement [8].



a



b



c

Напряжение (кВ): 20.00				
Сумма формульных коэффициентов: 10				
Сумма %: 100.00				
Элемент	Инт.	С %	Атом. %	
Al	K	6841	5.61	12.549
Cr	K	6733	6.66	7.725
Co	K	10189	11.68	11.954
Ni	K	38821	60.51	62.179
Mo	L	802	1.44	0.907
Hf	L	203	1.50	0.508
Ta	L	533	7.92	2.641
W	M	4312	4.68	1.537

d

Fig. 1. The microstructure (*a*, *b*, *c*) and chemical composition (*d*): *a* – alloy IC10 along the axis; *b* – alloy IC10 across the axis; *c* – analog M2 to alloy IC10; *d* – analog M2 to alloy IC10 by area; «Напряжение (кВ)» – Voltage (kV); «Сумма формульных коэффициентов» – Sum of formula coefficients; «Сумма %» – Sum %; «Элемент» – Element; «Инт.» – Intensity; «Атом. %» – At. %

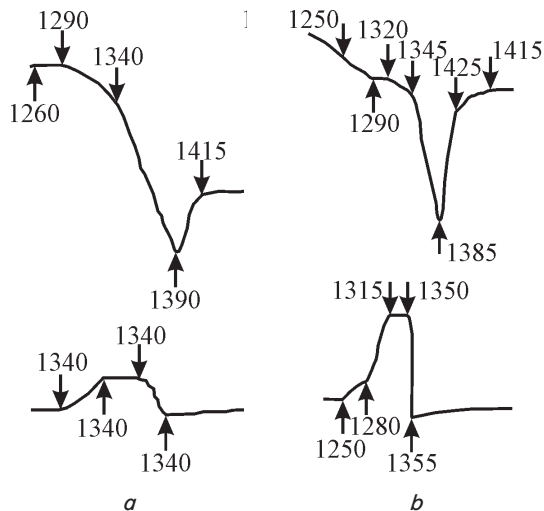


Fig. 2. Thermograms after thermal treatment: a – alloy IC10 (PRC); b – smelted analog M2

To assess the effect of rhenium on the IC10 alloy thermal characteristics, three ingots were melted at this stage of our research; they contained 1.0; 2.5; and 4.0 % by weight of Re. Data from the differential thermal analysis confirmed a significant increase in the liquidus temperature of alloys (~5 °C per 1 % by weight of Re). For the alloy containing 4.0 % by weight of Re, the melting point reaches 1,405 °C (Fig. 3).

To reduce the temperature of liquidus and solidus, as well as to form the γ' -phase, the alloy IC10 was introduced with Ti in the amount of 4.5–5.5 % by weight, which is used in the HNA filler metals, together or instead of Nb [13, 18, 19, 32].

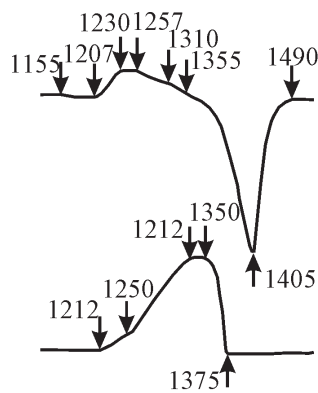


Fig. 3. Thermogram of the IC10 alloy doped with Re in the amount of 4.0 % by weight

The embrittlement of HNA is caused by the formation of topologically densely packed (TDP) phases. Of the known triple and quadruple state diagrams, the γ -phase is adjacent to one of the following two-phase regions: $\gamma+\sigma$, $\gamma+\mu$, $\gamma+R$, $\gamma+P$, where σ , μ , R , P are the TDP phases. They bind a significant amount of base alloying refractory metals and lean the γ -phase with them. Their evolution in the form of plates (Fig. 4) occurs at temperatures 1,150–1,200 °C during thermal treatment or during operation.

Taking into consideration the danger of the evolution of TDP phases, the PHACOMP software computed the compositions of 36 alloys for the filler metal base, 18 of which were subjected to differential thermal analysis. The main estimation parameters were the amount of γ' -phase, the dis-

tribution of elements for the γ - and γ' -phases, the difference in the parameters of the lattices of the γ - and γ' -phases (misfit), the number of vacancies in the alloy, the temperatures of liquidus, solidus, and solvus.

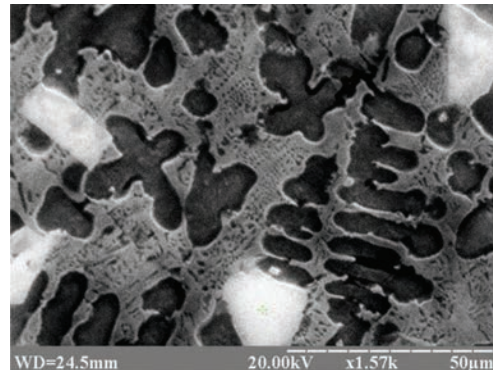


Fig. 4. Evolution of topologically densely packed intermetallide phases

The calculations confirmed the hardening of the solid solution by the Cr, Co, Mo, W, Re elements, and the dispersion strengthening – by Al, Ti, Ta, Hf. The distribution ratios of the alloying elements between the γ' - and γ -phases is less than unity for all the elements stabilizing the γ -phase, and exceeds unity for those stabilizing the γ' -phase. In all alloys, K_{Re} does not exceed 0.12. The amount of the γ' -phase varied from 61.3 to 71.4 %, depending on alloying.

In addition, our calculations showed the excessive alloying of some alloys with Cr, Mo, W, Re, which increase the number of electron vacancies in the alloy. The largest number of electron vacancies is demonstrated by W – 4.66 (for Re, 3.66), so its concentration at the filler metal base was reduced to 1.5–3.5 % by weight compared to the IC10 alloy. The Cr concentration was increased by 3 % by weight as the tests of the experimental samples of the filler metal revealed an increased rate of high-temperature corrosion. Taking into consideration the influence of rhenium on HNA strength, its concentration at the filler metal base was accepted to be 2.0–4.0 % by weight. The concentrations of the rest of the elements are close to the composition of the IC10 alloy.

By comparing the calculation results, the data from VDTA, as well as the recommendations given in [29–31], we optimized the chemical composition of the filler metal base (% by weight): (10.5–12.5) Cr; (7.0–10.0) Co; (3.0–5.) Al; (2.0–4.0) Ta; (2.0–4.0) Re; (1.5–3.0) W; (1.0–2.0) Mo; (1.0–2.0) Hf; (4.5–5.5) Ti; Ni is the rest; it was termed SBM-3.

5. 2. Choosing a depressant for the filler metal SBM-3

The successful use of zirconium as a filler metal depressant for the IC10 alloy was noted by the authors of paper [33]. Using the system Ni_(alloyed)-Hf-Zr, they performed a diffusion welding involving a liquid eutectic layer, which was easily removed from the joint under pressure on activating the joined surfaces. However, when the clearance increased to 0.08–0.1 mm, it was not possible to get rid of the eutectic layer in the seam even though the depressant concentration was reduced to 2.0 % [15]. It should also be noted that the use of zirconium in the amount exceeding 5.0 % requires strict control over the inflow into the vacuum chamber to avoid the oxidation of zirconium, which forms a black oxide film at the surface of the filler metal.

The application of silicon as a depressant when brazing the alloy IC10 is also impractical as its content in the alloy IC10 is limited to 0.2 % by weight Palladium alloying and its effect on the structure and properties of heat-resistant alloys have not been studied in detail.

The most studied and described in the scientific literature are the filler metals that involved boron as a depressant [13, 18, 19, 22, 32].

A positive feature of boron is its high diffusion mobility and the formation of highly-dispersed borides. It should be noted that the filler metals with boron wet well the alloy IC10 while filling almost zero clearances at which the eutectic layer at the top of the corner is absent. The joint is not detected at a clearance of up to 0.02–0.025 mm. In terms of the microstructure it is similar to the joint in diffusion welding with a melting layer, although the pressure was not applied to the samples.

The disadvantage of boron as a depressant is the possibility of the formation of fusible boride eutectics, which are located in the central part of the seam.

Summing up the above, it is advisable to use boron as a depressant for the filler metal SBM-3. The IC10 alloy, doped with rhenium, was used as the filler metal base. Smelting the filler metal involved the NB1 ligature, containing boron in the amount of 10.5 % by weight, and not more than 0.005 S; 0.009 P; 0.05 Si; 0.05 Al; 0.08 C. The amount of the ligature introduced was calculated depending on the content of boron in the alloy being melted. The boron content was experimentally determined by a method of atomic emission spectral analysis. Initially, the filler metal samples containing boron in the amount of 0.7; 1.0; 1.5; 2.0; and 2.5 % by weight were smelted. The analysis of data from electron microscopy and differential thermal analysis allowed us to narrow the interval of boron concentration from 0.7 to 1.5 % by weight

The base of MC carbides is tantalum, titanium, and hafnium. The $M_{23}C_6$ -type carbides are formed on the basis of chromium, molybdenum, and tungsten.

It was proven in [34] that various elements of the alloying complex exert an ambiguous effect on the temperature of phase transformations in complexly-doped heat-resistant nickel alloys. Thus, it was experimentally established that Ti, Al, Ta, Hf, Zr, W, Mo positively affect T_γ , that is, increase the thermal stability of the γ' -phase and the alloy in general, while So, Cr, V, and C reduce T_γ . Some difference in the temperature values of phase transformations in our study and in that reported in [34] could be explained by the mismatch between the ratios of the content of the elements of the alloying complex; however, the order of melting and phase crystallization holds.

Boron significantly reduces the thermal stability of the γ' -phase and the alloy in general. In addition, the alloys form the $\gamma+Ni_3B$ eutectics with a rather narrow crystallization interval. Temperatures of the beginning of melting and the beginning of crystallization of these eutectics, regardless of the amount of boron injected into the alloy, are almost identical within the error margin of the method (the eutectics temperature in the Ni-B system is 1,093 °C [35]).

Regardless of the amount of boron injected into the alloy, the temperature of the unbalanced solidus (or the local melting of the eutectic phase $T_{\gamma+\gamma'}$) does not change. As the boron content increases, the temperature of melting completion is also significantly reduced.

The SBM-3 alloy in its original state is characterized by a homogeneous dispersed ($\gamma+\gamma'$)-structure with a high volume share of the hardening γ' -phase (68±70 % by volume). The particles of the γ' -phase have a characteristic cube-type shape, the size of 0.3±0.4 μm (Fig. 5, *a*). Doping the alloy with boron has led to a significant change in its structure (Fig. 5, *b*). In the cross-section, metallographic thin sections clearly demonstrate a dendritic structure with the formation of large eutectic precipitates ($\gamma+\gamma'$) in the inter-dendrite regions.

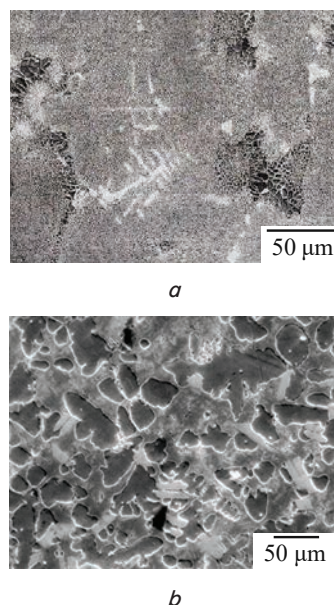


Fig. 5. Structure of the alloy SBM-3: *a* – in its original state; *b* – doped with 1.1 % B

It is known from [34, 36] that in HNA with multi-component alloying there is a significant change in the morphology and composition of carbide phases whose number increases dramatically with the introduction of hafnium and boron [37]. Carbide phases can coexist in HNA with an equiaxial dendritic structure: based on the monocarbides of titanium, niobium, tantalum, and hafnium (MS); based on chromium carbides ($M_{23}C_6$); complex carbides based on refractory metals W, Mo, and nickel (M_6C).

Carbide phases of the $M_{23}C_6$ type are formed mainly on the periphery of the dendrites' branches and grains' boundaries, reaching the sizes of 200–300 μm^2 . Their surrounding with the plastic γ' -phase prevents the embrittlement of alloys and increases the resistance to the grain-boundary slip.

The M_3B boride phases (where M – Mo, W, Ti, Cr, Ni, So) in the form of grain-boundary precipitations could grow from the border deep into the grain. Located in the joints of lattices of different orientations, they increase the resistance to deformation creep [35, 38].

5.3. Studying the surface properties of filler metals and their interaction with the IC10 alloy

The next step in optimizing the depressant composition for SBM-3 filler metal was to study the formation of a brazed joint at temperatures of 1,250 and 1,260 °C on wedge samples with a constant clearance at a certain time of brazing. The brazing temperatures were selected according to the data from differential thermal analysis. We used the filler

metals containing rhenium in the amount of 2.0–4.0 % by weight. The criterion for the most favorable concentration of boron was the absence of the eutectic layer in the middle of the seam at a clearance of 0.08–0.1 mm.

The formation of the brazed joint and its structure is largely determined by the magnitude of the maximum and minimum clearances. The clearance in the wedge samples was made with the help of tungsten wire with a diameter of 0.3 or 0.6 mm (Fig. 6, *a, b*).

The wire was installed on one side between the connected plates. On the other side, at the top of the corner (Fig. 6, *c*), a joint between the filler metal and the chemical composition of the main metal is formed. With a changing clearance of 0.08–0.12 mm (Fig. 6, *d*), the amount of filler metal is sufficient for the volume interaction with the main metal and its dissolution.

The melted filler metals were experimentally examined for wetting the IC10 alloy and flowing in a vacuum no worse than 5×10^{-3} Pa. The inflow magnitude provided did not exceed 3×10^{-5} Pa \times m³s⁻¹, which warrants the activation of the surface of the heat-resistant alloy at temperatures above 1,150 °C [12]. The brazing temperature aging time in all cases was 20 minutes.

We studied the impact exerted by the technique to prepare the IC10 alloy surfaces to brazing. We used mechanical sanding at the machine and polishing by hand on a fine emery cloth H-0. It was established that at a temperature of 1,260 °C the specific area of filler metal spread that contains Re in the amount of 2.5 % is 15–20 % larger at machining than that at manual treatment (Fig. 7, *a, b*).

Further studies were carried out using samples of the IC10 alloy with a mechanically polished surface (Fig. 8). The specific area of the spread was determined for filler metals containing Re in the amount of 2.5 and 4.0 % by weight, at temperatures 1,235, 1,250, and 1,260 °C.

At 1,250 °C, S_{spec} is approximately 2.0 mm²/mg at a rhenium content of 2.5 % by weight, and 1.7–1.9 mm²/mg at its content of 4.0 % by weight (Fig. 7, *c, d*), which does not affect the quality of the brazing. At 1,260 °C, there is no difference in the spread. At 1,235 °C, the brazing spread area is much smaller (Fig. 7, *d*).

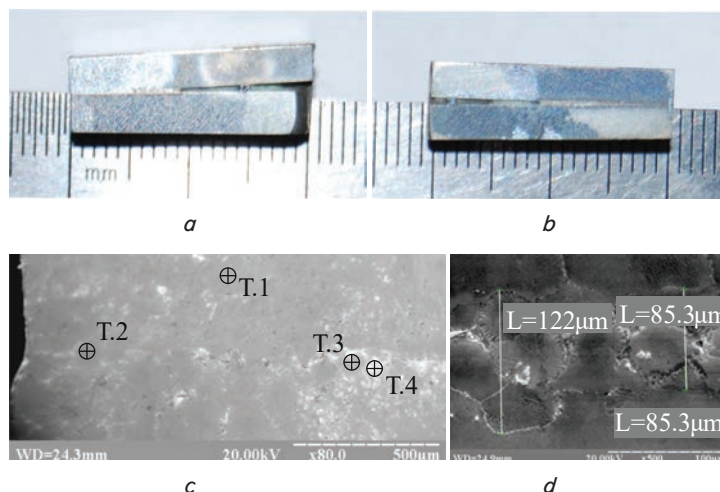


Fig. 6. Wedge samples (*a, b*), filling the clearance (*c*) with the filler metal, and the microstructure of the IC10 alloy joint when brazing using SBM-3 filler metal (*d*): *a* – with a wire diameter of 0.6 mm; *b* – with a wire diameter of 0.3 mm; *c* – at the top of the corner, x100; *d* – with a changing clearance of 0.085–0.122 mm, x250

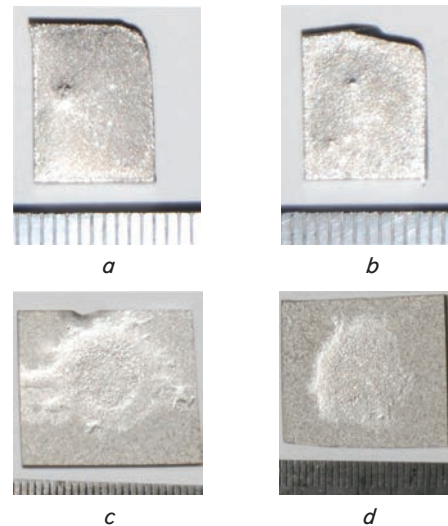


Fig. 7. The spread of the IC10 alloy batch at 1,250 °C: *a* – 50 mg, containing Re in the amount of 2.5 %, on the polished surface; *b* – 50 mg, containing Re in the amount of 2.5 %, on the surface treated by the emery cloth H-0; *c* – 100 mg, containing Re in the amount of 2.5 %; *d* – 100 mg, containing Re in the amount of 4.0 %

The wetting ability of the filler metal, characterized by the contact angle of wetting, determines its spread on the surface of the main metal, the work of the adhesion of the melt, and depends on the energy of surface tension. The value of surface energy (surface tension) was determined by a method of the underlying drop [13]. This method usually involves a ceramic substrate, which is not wetted by melt. Since the melted filler metals wet ceramics well, we used boron carbonitride boron as a substrate. The contact angles of wetting were determined by the macro-sections obtained after cutting the plates by the diameter of the spread drop (Fig. 9).

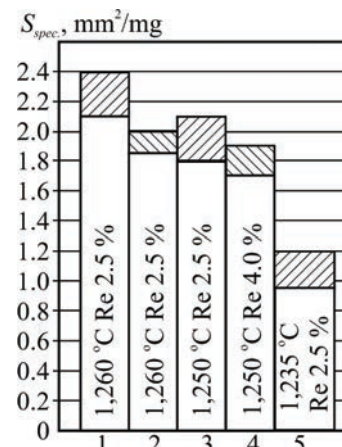


Fig. 8. The specific area of the SBM-3 filler metal spread at temperatures 1,260, 1,250, 1,235 °C: 1 – on a polished surface; 2, 3, 4, 5 – on the surface treated by the emery cloth H-0

The contact angles of wetting the IC10 alloy with the filler metal containing Re in the amount of 4.0 %, at 1,250 and 1,260 °C, are 7.0–8.0° and 5.0–6.0°, respectively. Values for the filler metal containing 2.5 % of Re are similar, within the measurement accuracy, to those for the filler metal containing Re in the amount of 4.0 %.

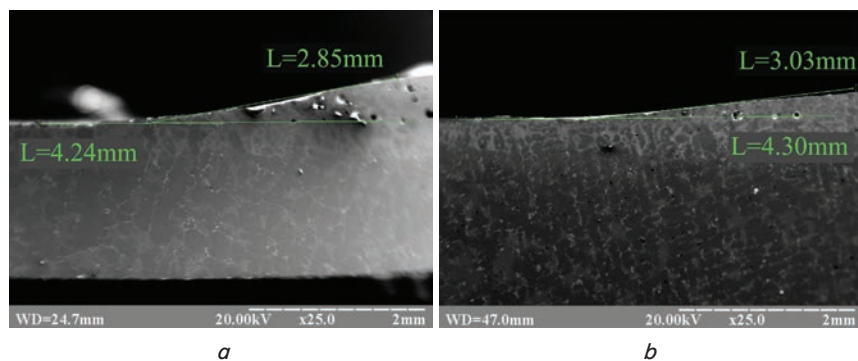


Fig. 9. Contact angles of wetting the IC10 alloy with the filler metal containing Re in the amount of 4.0 %: *a* – at 1,250 °C; *b* – at 1,260 °C

5.4. Studying the structure, chemical composition, and properties of brazed joints

The dissolution of the main metal depends on a series of factors [13]. It was established that regardless of the content of boron (up to 1.3 % by weight), at brazing temperatures above 1,270 °C, the depth of dissolution of the IC10 alloy increases intensively, which does not make it possible to control the width of the seam. Therefore, the brazing temperature should not exceed 1,260 °C (the temperature of homogenization of the alloy IC10). In this case, the depth of dissolution of the main metal does not exceed 0.1 mm, and, in the fusion zone, during the brazing, there form common grains between the main metal and the seam (Fig. 10).

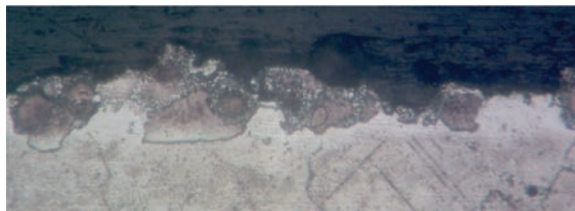


Fig. 10. Formation of a transition zone between the main metal and the seam when brazing the alloy IC10 with the filler metal SBM-3; $\times 250$

When using a filler metal containing boron in the amount of 0.8–1.2 % by weight, the structure of the main metal and the seam is identical. After brazing and thermal treatment, there is no boride eutectic in the joint. The high diffusion mobility of boron atoms contributes to the isothermal crystallization of filler metal, as well as the release of dispersed borides in the transition area. Carbide and boride inclusions are characterized by high concentrations of active elements to carbon and boron, which are clearly highlighted on spectra. All such inclusions have a low concentration of aluminum. In some phases, the concentration of Ta, W, and Ti is high.

It has been established that after thermal treatment the main metal and the brazed seam have a homogeneous dispersed structure ($\gamma+\gamma'$ -phase). The volume of the hardening γ' -phase is 70 %, its particles have a characteristic cuboid shape of 0.3–0.4 μm (Fig. 11).

The brazed seam has a width of about 0.08 mm. Its structure is almost no different from the original structure of the alloy IC10. The section of the brazed seam is cut out of a sample that collapsed beyond the joint during the high-temperature tests for strength.

Fig. 12 shows the microstructure of the brazed joint, which has the marked points of the chemical analysis of the main metal (1, 8, 10) and the metal of the brazed seam (the rest). The

concentrations of elements at the analysis points are given in Table 2.

There are several characteristic points in the microstructure, such as point 9, with the high Cr, Re, Mo, W, and low Ni content. At points 7 and 3, there is a high concentration of Ta, W, Ti, and low Cr, Co, without Re. In the filler metal matrix, the concentration of Re varies from 0.24 to 3.24 %. Some phases could be distinguished by coloration in chemical etching; however, identifying them requires a thorough X-ray structure analysis.

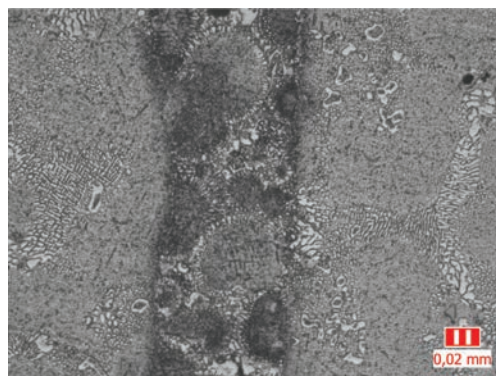


Fig. 11. Microstructure of the joint when brazing the alloy IC10 with the filler metal SBM-3

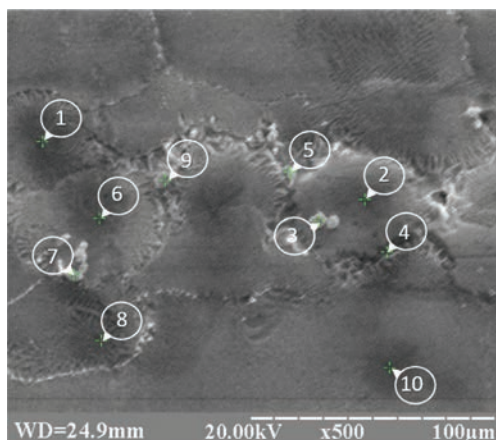


Fig. 12. The microstructure of the joint when brazing the alloy IC10 with the filler metal SBM-3 showing the points of local X-ray spectral microanalysis

In brazed joints, the chemical composition of the metal was determined, both at individual points and by areas of the brazed seam at different magnification. An increase in the magnification leads to a decrease in the area scanned on the sample under study and its localization. Fig. 13 shows the spectrogram and Fig. 14 the results from the analysis by area at their various magnification.

The average concentration of elements across the three zones is (% by weight): 3.44 Al; 5.5 Ti; 10.6 Cr; 6.55 Co; 63.3 Ni; 0.95 Mo; 1.66 Hf; 2.8 Ta; 2.8 W; 1.6 Re; B and C – not defined. All elements are in the concentrations that correspond to their interval change in the SBM-3 filler metal. The lower concentration of rhenium is due to its increased concentration in carbides containing chromium, tungsten, and molybdenum.

Table 3

The strength limit σ_B^0 of the alloy IC10 and the brazed joints σ_B^c at stretching the cylindrical samples at a temperature of 1,100 °C

No. of entry	Material	Strength limit, MPa		σ_B^c / σ_B^0
		Alloy IC10, σ_B^0	Joint, σ_B^c	
1	Base metal, IC10	275	–	–
2	Filler metal BH-3#, clearance 0.08 mm	–	169	0.62
3	Filler metal BH-3#, clearance 0.03 mm	–	252	0.92
4	Filler metal SBM-3, clearance 0.08 mm	–	268	0.98

Table 4

The durability of the IC10 alloy and the brazed joints when testing cylindrical samples for stretching at 1,100 °C

No. of entry	Material	Tension, MPa	Durability, h	
			Required	Actual
1	Base metal, IC10	36	≥100	102
2	Filler metal BH-3#, clearance 0.08 mm		≥100	18.97
3	Filler metal BH-3#, clearance 0.03 mm		≥100	66.17
4	Filler metal SBM-3, clearance 0.08 mm		≥100	102

5. 5. Development of the IC10 alloy brazing technology

The process technology consists of a sequence of certain operations during the preparation of joined surfaces, technological materials, assembly, brazing, and the finishing of an article or sample. The technological materials, in this case, include a filler metal in the form of powder and acrylic resin that fixes the filler metal at the edge of the clearance. The size of the clearance is provided by the tungsten thread of the required diameter, which is fixed by capacitor welding. The joint surface prior to brazing is treated by polishing in the direction of the filler metal inflow. Before assembly, the joined surfaces are wiped with alcohol. No other means of additional surface cleaning or activation are used.

The brazing is performed in a vacuum no worse than $5 \cdot 10^{-3}$ Pa under careful control over the inflow amount. The brazing temperature is 1,250–1,260 °C with an aging of 20 minutes. This technology was used to fabricate the samples for the mechanical testing of the joints.

The mechanical tests of the brazed joints were carried out after a thermal treatment. The thermal treatment mode was determined by the dissolution curves of the γ' -phase, the carbide and boride phases, built by the software JMatPro: aging at 1,180 °C – 2.5 hours; 1,065 °C – 2.5 hours. The tests of the IC10 alloy joints using the SBM-3 filler metal, at a clearance of 0.08 mm, were conducted in the PRC (CEPREI).

6. Discussion of results of studying the structure, composition, and properties of the filler metal and brazed joints

Modern heat-resistant nickel alloys are complex multi-element systems whose properties are determined by a set of thermodynamic processes. Introducing new elements or changing the content of existing ones could lead to the transformation of the existing or the formation of new undesirable phases. For example, high concentrations of elements that harden a solid solution (W, Mo, Cr, Re, and others) could give rise to topologically densely-packed (TDP) phases. These are the electron intermetallic compounds. The possibility of their formation is determined by the number of elec-

tron vacancies n_v in the solid solution. Alloys contain a series of elements with a high affinity for carbon, boron, forming carbides and borides, which affect the intermetallics' hardening (forming the γ' -phase) and several other processes. To evaluate these processes, the PHACOMP software identifies dozens of parameters. These parameters include the number and the grid parameters of the γ and γ' -phases. The software determines the efficiency of alloy hardening, the number of electron vacancies n_v , the critical value n_{vc} , the quantity of carbides, borides, the distribution of elements in a solid solution and in the γ' -phase. It computes the temperatures of liquidus, solidus, and solvus, the concentration of each alloying element in the γ and γ' -phases, the temperature factor of linear expansion, density, creep rate, the corrosion rate in fuel combustion products. The JMatPro software builds a graphical image of the change in the number of alloy phases depending on the temperature.

Modern alloys are over-doped. For example, if one takes the IC10 alloy as a base and adds Re in the amount of 4.0 %, then the corresponding n_v window would show: "Attention! TCP – Dangerous!", which that warns of the occurrence of the σ -phase (Fig. 4). In this case, one needs to reduce the content of the element with a high number of electron vacancies. This element is tungsten. Therefore, part of tungsten is replaced with rhenium, which is a more effective hardener. Similarly, other parameters are used to ensure optimal alloying, for example, to reduce creep and corrosion rates.

In our work, we estimated 36 possible options for alloying the base of a filler metal; it is very labor-consuming to experimentally investigate them. Based on the calculations and experimental studies, we have chosen the following chemical composition (% by weight): 10.5–12.5) Cr; (7.0–10.0) Co; (3.0–5.0) Al; (2.0–4.0) Ta; (2.0–4.0) Re; (1.5–3.0) W; (1.0–2.0) Mo; (4.5–5.5) Ti; the rest is nickel. Choosing a filler metal depressant by computer simulation is not currently possible as the required volume of statistical data is not available. Taking into consideration our experimental studies, the results reported in the cited works, as well as the features of the IC10 alloy, we have non-alternatively chosen boron as a depressant. It was noted above that a series of experiments was carried out to determine the optimal amount

of boron, from 0.7 to 2.5 % by weight. As well as multilateral studies in a concentration interval of 0.7 to 1.5 %. The study results have shown that the filler metal containing boron in the amount of up to 1.3 % has no eutectic layer when filling wedge clearances in the center of the brazed seam (Fig. 6). The filler metal wets well and spreads across the surface of the IC10 alloy (Fig. 7–9). The microstructure of the brazed joint is homogeneous in both the seam and the transition zone (Fig. 10–12). After thermal treatment, the main metal and the brazed seam have a highly-dispersed structure and a similar chemical composition (Table 2, Fig. 14). The thermogram of the filler metal, termed SBM-3, is shown in Fig. 15.

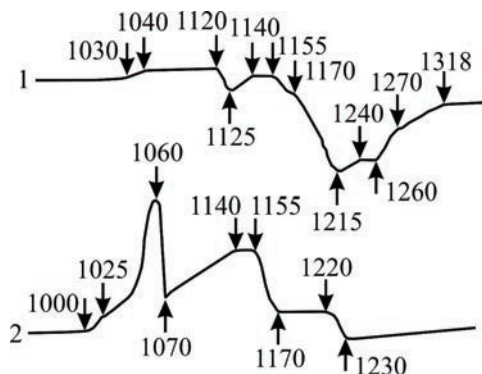


Fig. 15. Thermogram of the filler metal SBM-3 containing B in the amount of 1.1 %: 1 – heating; 2 – cooling

A special feature of the proposed method of filler metal design is the selection of two stages. In the first stage, the filler metal base is chosen, which makes it possible to use the achievements of the metal science of heat-resistant alloys and their doping. This employs computer methods for calculating the resulting phases, their composition, critical temperatures, and other characteristics, including physical and mechanical ones. In the first stage, the IC10 alloy containing 2.4 % of tantalum was selected as the base of the filler metal. It is known [30] that rhenium is more effective at strengthening the γ -phase than tungsten; tantalum participates in dispersion hardening. The concentration of 2.0–4.0 % of rhenium is due to that at high concentrations the alloy may be prone to the formation of unstable releases of the γ -phase. For a balanced alloying of the filler metal base with refractory metals, one reduces the concentration of tantalum, to ensure the ratio of Ta to W to be close to unity [1, 30, 39]. Since the number of rhenium electron vacancies (3.66) is less than that of tungsten (4.66), the resistance of the alloy of the filler metal base to embrittlement increases.

To enhance the casting properties, the IC10 alloy contains 1.0–2.0 of hafnium, which could also affect the temperature of the filler metal's liquidus. Since hafnium has a high affinity for carbon and boron, forming the refractory carbides and borides, it has no significant effect on the reduction of the liquidus temperature. The formation of HfC carbide when brazing the alloy IC10 with the filler metal BH2 was also established in work [4].

In the second stage, a depressant is selected, based on the experimental methods for studying its interaction with the filler metal base and the main metal. The SBM-3 filler metal contains boron in the amount of 0.8–1.2 % by weight.

The alloying of the filler metal base by boron leads to a significant change in temperatures, both melting and crystallization. In alloys, the γ +Ni₃B eutectics form with a narrow

crystallization interval. The temperatures of the beginning of melting and the beginning of crystallization of the eutectics are almost identical regardless of the amount of boron introduced; the solidus temperature does not change either. The emergence of the boride eutectics also affects the melting of the carbide eutectics. For the original alloy, the heat thermogram clearly distinguishes the effects of melting the γ -dendrites and carbide eutectics. In the thermogram of the alloy containing boron in the amount of 1.0 % by weight, these temperatures are almost the same. With the increase in the boron content to 1.3 %, the γ +MC melting interval is narrowed; both effects merge, respectively, the melting completion temperature decreases.

Primary carbides of the MC type (volume share, 6.0–10.0 %) form at crystallization in the form of large (15–40 μ m) randomly located particles of cubic or skeletal morphology. There is a preferred order for the formation of these carbides corresponding to the affinity of metals to carbon: Ti, Hf, Zr, Ta, Nb [38]. Molybdenum and tungsten could partially replace metals in these carbides, forming the phases of type (Ti, Mo, W) C; (Ti, Hf, Mo, W) C, and others. Given the presence of titanium, hafnium, and tantalum in the IC10 alloy and the SBM-3 filler metal, it is possible to assume the formation of their primary carbides in the seam, which confirms the presence of inclusions with a high concentration of these elements in it.

The MC carbides, formed from the melt during an alloy crystallization, may undergo transformation into other types of carbides in accordance with the following solid-phase reactions: $MC + \gamma \rightarrow M_{23}C_6 + \gamma'$; $MC + \gamma \rightarrow M_6C + \gamma'$. The $M_{23}C_6$ carbides are stable up to temperatures of 750–790 °C. More stable are double carbides of the M_6C type, which are formed in heat-resistant alloys with a high content of refractory metals and are characterized by the wide ranges of compositions within the $M_3C - M_{13}C$ limits. Typical double carbide compositions are (Ni, Co)₃Mo₃C, (Ni, Co)₂W₄C, and Ni₃(W, Mo)₃C.

The main task to be solved in this work was to make the brazed joints of the IC10 alloy, which would possess the short-term and long-lasting strength of at least 80 % of the strength of the main metal at a clearance of 0.08 mm. The tests of the brazed joints in the PRC showed that the set task was solved (Tables 4, 5). At CEPREI, they simultaneously tested the main metal, the best filler metal BH-3# (PRC) at a clearance of 0.08 mm and 0.03 mm, as well as the SBM-3 filler metal at a clearance of 0.08 mm. As noted above, a 0.03 mm clearance forms a joint similar to that in the diffusion welding with a melting layer. Homogenization of the joint with a micron layer occurs due to diffusion. At the limited amount of the diffusing substance, the diffusion equation takes the following form [13]:

$$C_{(x,t)} = \frac{C_0 \cdot h}{2 \cdot \sqrt{\pi \cdot D \cdot t}} \exp\left(-\frac{x^2}{4 \cdot D \cdot t}\right), \quad (1)$$

and the concentration in the center of the layer, where the concentration of the depressant is maximum, is determined from the following equation

$$C_{(0,t)} = \frac{C_0 \cdot h}{2 \cdot \sqrt{\pi \cdot D \cdot t}}, \quad (2)$$

where $C_{(x,t)}$ and $C_{(0,t)}$ is the concentration of a depressant at any point with coordinate x over time t and in the center of the layer respectively; D is a diffusion factor; C_0 is the initial concentration of a diffusing substance; h is the thickness of the layer.

The necessary data for specific calculations of boron diffusion (the energy of diffusion activation and the diffusion ratios) are given in paper [4].

Equations (1), (2) show that the thicker the layer, the longer it takes to absorb the depressant by diffusion. This time is proportional to the square of the thickness of the layer. At capillary brazing (0.05–0.10 mm), the time of homogenization, depending on the permissible concentration of a depressant in the center of the layer, is several days. At a diffusion welding with a melting layer, due to the pressure, this time is minutes, as the residual magnitude of the layer after the compression pressure application is a fraction of the micron. Therefore, to achieve mechanical properties close to the properties of the main metal, one requires a minimum concentration of the depressant, the development of special filler metals and technologies. At TLP-Bonding, there is an isothermal crystallization of the melt.

The results from Tables 3, 4 confirm the above statement. At a clearance of 0.08 mm, the filler metal BH-3# demonstrates a strength limit of 169 MPa, and at a clearance of 0.03 mm – 252 MPa. Such a pattern is also confirmed by its durability.

The SBM-3 filler metal ensures the mechanical properties of joints close to the properties of the main metal at 1,100 °C. The tensile strength of the joints is 98 % of the strength of the base metal and meets the requirements for durability at the level of requirements for the base metal (102 hours).

The SBM-3 filler metal is designed for brazing the cast nozzle blades made from the IC10 alloy with a directional or monocrystalline structure. It could be used for brazing other similar alloys of the same type. The brazing is performed at a temperature of 1,250–1,260 °C in a vacuum no worse than $5 \cdot 10^{-3}$ Pa in furnaces with a heating of up to 1,500 °C. The aging time at the brazing temperature is 20 minutes.

The filler metal could be used to braze the blades into a package, to correct surface casting defects, to braze the holes in cooled blades for fixing ceramic rods.

The SBM-3 filler metal could also be used for brazing the casting nickel heat-resistant alloys that allow heating to a temperature of 1,250–1,260 °C.

The advantage of SBM-3 filler metal is ensuring the strength of joints close to the main metal at a clearance of 0.08 mm, which is required for assembling parts with a sliding landing.

The prospects for the developments outlined in this paper are confirmed by the creation of a new filler metal SBM-4 (based on the SBM-3 filler metal) for brazing heat-resistant alloys in the next generation of marine gas turbines.

7. Conclusions

1. This work proposes a procedure for designing filler metals in two stages. The first stage is the choice of the filler metal base, which should be close in composition to the brazed alloy, taking into consideration its features. This stage involves computer software, which makes it possible to significantly reduce the amount of experimental work (estimation stage). The second stage is to study the interaction between the filler metal with introduced depressants and the main metal (experimental stage) and to accumulate statistical data for software processing.

2 The chosen base of the SBM-3 filler metal is the following system, % by weight: (10.5–12.5) Cr; (7.0–10.0) Co; (3.0–5.0) Al; (2.0–4.0) Ta; (2.0–4.0) Re; (1.5–3.0) W; (1.0–2.0) Mo; (4.5–5.5) Ti; the rest is nickel. Boron (0.8–1.2 % by weight) was selected as a depressant.

3. It has been established that at brazing temperature the filler metal SBM-3 demonstrates high technological properties. The specific area of the spread is 1.9–2.0 mm²/mg, the contact angles of wetting are 5.0–8.0°.

4. Following thermal treatment, the main metal and the brazed joint possess a homogeneous, highly-dispersed structure, and close chemical composition. The volume of the hardening γ -phase is 70 %. The seam's metal demonstrates the high resistance to the embrittlement and high-temperature corrosion in fuel combustion products. Our studies have shown that the filler metal developed provides mechanical properties close to the properties of the main metal. The tensile strength of joints with the SBM-3 filler metal is 98 % (268 MPa) of the strength of the base metal, and meets the durability requirements at the level of requirements for the base metal (102 hours) at a test temperature of 1,100 °C.

5. We have devised a technology for brazing heat-resistant alloys based on Ni₃Al, specifically alloy IC10 with directional crystallization. The SBM-3 filler metal is made in a powder form. The brazing is performed in a vacuum no worse than $5 \cdot 10^{-3}$ Pa. The brazing temperature is 1,250–1,260 °C at an aging of 20 minutes.

Acknowledgments

We express sincere gratitude to the Foreign Economic Representation of the China-Ukrainian Welding Institute named after E. O. Paton for funding, attention, and assistance in our research.

References

1. Kablov, E. N., Petrushin, N. V., Sidorov, V. V. Rhenium in the thermally stable nickel alloys for single crystal blades of gas turbine engines. 7th International symposium on Technetium and Rhenium Science and Utilization. Available at: <https://docplayer.ru/49222411-Rhenium-in-the-thermally-stable-nickel-alloys-for-single-crystal-blades-of-gas-turbine-engines.html>
2. Kablov, E. N. (2012). Strategical areas of developing materials and their processing technologies for the period up to 2030. *Aviatsionnye materialy i tehnologii*, 8, 7–17.
3. Kablov, E. N., Ospennikova, O. G., Bazyleva, O. A. (2011). Materialy dlya vysokotekhnologicheskikh detaley gazoturbinnih dvigateley. *Vestnik Moskovskogo gosudarstvennogo tekhnicheskogo universiteta im. N.E. Bauman. Seriya «Mashinostroenie»*, SP2, 13–19. Available at: <https://cyberleninka.ru/article/n/materialy-dlya-vysokotekhnologicheskikh-detaley-gazoturbinnih-dvigateley>
4. Yue, X., Liu, F., Chen, H., Wan, D., Qin, H. (2018). Effect of Bonding Temperature on Microstructure Evolution during TLP Bonding of a Ni₃Al based Superalloy IC10. *MATEC Web of Conferences*, 206, 03004. doi: <https://doi.org/10.1051/mateconf/201820603004>
5. Intermetallic Alloy Development. A Program Evaluation (1997). Washington, DC: The National Academies Press. doi: <https://doi.org/10.17226/5701>

6. Buntushkin, V. P., Kablov, E. N., Bazyleva, O. A. (1995). *Mechanicheskie i ekspluatatsionnye svoystva liteynogo zharoprochnogo splava na osnove intermetallida Ni₃Al*. *Metally*, 3, 70–73.
7. Buntushkin, V. P., Bazyleva, O. A., Povarova, K. B., Kazanskaya, N. K. (1995). *Vliyanie struktury na mehanicheskie svoystva legirovannogo intermetallida Ni₃Al*. *Metally*, 8, 74–80.
8. Sims, Ch. T., Stoloff, N. S., Xagel, U. K. (1995). *Supersplavy II: Zharoprochnye materialy dlya aerokosmicheskikh i promyshlennykh energoustanovok*. Vol. 1. Moscow: Metallurgiya, 384.
9. Yushchenko, K. A., Makhnenko, V. I., Savchenko, V. S., Chervyakov, N. O., Velikoivanenko, E. A. (2007). Investigation of Thermal-Deformation State of Welded Joints in Stable-Austenitic Steels and Nickel Alloys. *Welding in the World*, 51 (9-10), 51–55. doi: <https://doi.org/10.1007/bf03266600>
10. Kvasnitskiy, V. F. (1986) *Svarka i Payka zharoprochnykh splavov v sudostroenii*. Leningrad: Sudostroenie, 222.
11. Kazakov, N. F. (Ed.) (1985). *Diffusion Bonding of Materials*. Moscow: Mir Publishers, 312.
12. Krivtsun, I. V., Kvasnytskyi, V. V., Maksymov, S. Yu., Yermolaiev, H. V.; Paton, B. Ye. (Ed.) (2017). *Spetsialni sposoby zvariuvannia*. Mykolaiv: NUK, 346.
13. Yermolaiev, H. V., Kvasnytskyi, V. V., Kvasnytskyi, V. F., Maksymova, S. V., Khorunov, V. F., Chyharov, V. V.; Khorunov, V. F., Kvasnytskyi, V. F. (Eds.) (2015). *Paiannia materialiv*. Mykolaiv: NUK, 340.
14. Petrushynets, L. V., Falchenko, I. V., Ustinov, A. I., Novomlynets, O. O., Yushchenko, S. M. (2019). Vacuum Diffusion Welding of Intermetallic Alloy γ -TiAl with High-Temperature Alloy EI437B Through Nanolayered Interlayers. 2019 IEEE 2nd Ukraine Conference on Electrical and Computer Engineering (UKRCON). doi: <https://doi.org/10.1109/ukrcon.2019.8879918>
15. Kvasnytskyi, V. V., Myal'nitsa, G. F., Matviienko, M. V., Buturlya, E. A., Chunlin, D. (2019). Investigation of interaction of Ni₃Al-based alloy with interlayers of different alloying systems for TLP-bonding. *The Paton Welding Journal*, 8, 12–17. doi: <https://doi.org/10.15407/as2019.08.03>
16. Zhang, H. R., Ghoneim, A., Ojo, O. A. (2010). TEM analysis of diffusion brazement microstructure in a Ni₃Al-based intermetallic alloy. *Journal of Materials Science*, 46 (2), 429–437. doi: <https://doi.org/10.1007/s10853-010-4884-7>
17. Zeng, K., Jin, Z. (1990). Optimization and calculation of the Hf-Ni phase diagram. *Journal of the Less Common Metals*, 166 (1), 21–27. doi: [https://doi.org/10.1016/0022-5088\(90\)90362-n](https://doi.org/10.1016/0022-5088(90)90362-n)
18. Lukin, V. I., Ryl'nikov, B. C., Afanas'ev-Hodykin, A. N., Timofeeva, O. B. (2013). *Osobennosti tehnologii diffuzionnoy Payki zharoprochnogo splava EP975 i liteynogo monokristallicheskogo intermetallidnogo splava VKNA-4U primenitel'no k konstruksii «Blisk»*. *Svarochnoe proizvodstvo*, 7, 19–25.
19. Ryl'nikov, V. S., Afanasiev-Khodykin, A. N., Galushka, I. A. (2013). Technology of braze design type «Blisk» from dissimilar alloys. *Trudy VIAM*, 10. Available at: <http://viam-works.ru/plugins/content/journal/uploads/articles/pdf/251.pdf>
20. Malashenko, I. S., Kurenkova, V. V., Belyavin, A. F., Trohimchenko, V. V. (2006). *Kratkovremennaya prochnost' i mikrostruktura payanykh soedineniy splava VZhL12U, poluchennykh s ispol'zovaniem borsoderzhashchego pripoya s prisadkoy kremniya*. *Sovremennaya elektrometallurgiya*, 4, 26–42.
21. Malashenko, I. S., Kurenkova, V. V., Onoprienko, E. V., Trohimchenko, V. V., Belyavin, A. F., Chervyakova, L. V. (2007). Mechanical properties and structure of brazed joints of cast nickel alloy ZhS26VI. Part 1. *Sovremennaya elektrometallurgiya*, 1, 25–32. Available at: <http://dspace.nbu.gov.ua/handle/123456789/95519>
22. Malashenko, I. S., Mazurak, V. E., Kushnareva, T. N., Kurenkova, V. V., Zavidonov, V. G., Yavdoshchina, E. F. (2014). *Payka v vakuume litogo nikelvego splava ZhS6U kompozitsionnymi pripoyami na osnove VPr-36. Chast' 1*. *Sovremennaya elektrometallurgiya*, 4, 49–58. Available at: <https://patonpublishinghouse.com/sem/pdf/2014/pdfarticles/04/9.pdf>
23. Belyavin, A. F., Kurenkova, V. V., Malashenko, I. S., Grabin, V. V., Trohimchenko, V. V., Chervyakova, L. V. (2010). *Prochnost' i mikrostruktura Payanykh soedineniy splava ZhS6U, poluchennykh s ispol'zovaniem bor- i borkremniysoderzhashchih pripoev*. *Sovremennaya elektrometallurgiya*, 2, 40–51. Available at: <https://patonpublishinghouse.com/sem/pdf/2010/pdfarticles/02/10.pdf>
24. Kurenkova, V. V., Malashenko, I. S. (2008). High-temperature brazing of high-temperature casting alloys by boron containing braze alloy doped with silicon. *Adgeziya rasplavov i payka materialov*, 41, 63–87. Available at: <http://dspace.nbu.gov.ua/handle/123456789/4378>
25. Afanas'ev-Hodykin, A. N., Lukin, V. I., Ryl'nikov, V. S. (2010). *Tehnologiya polucheniya nerazemnykh soedineniy iz splava ZhS36*. *Svarochnoe proizvodstvo*, 7, 27–31.
26. Lukin, V. I., Ryl'nikov, V. S., Afanas'ev-Hodykin, A. N., Orehov, N. G. (2012). *Osobennosti payki monokristallicheskih otlivok iz splava ZhS32*. *Svarochnoe proizvodstvo*, 5, 24–30. Available at: <https://elibrary.ru/item.asp?id=18820125>
27. Maksimova, S. V., Horunov, V. F., Myasoed, V. V., Voronov, V. V., Koval'chuk, P. V. (2014). *Mikrostruktura payanykh soedineniy alyuminidov nikelya*. *Avtomaticheskaya svarka*, 10, 17–23. Available at: http://nbuv.gov.ua/UJRN/as_2014_10_4
28. Maksymova, S. V., Voronov, V. V., Kovalchuk, P. V. (2017). Brazing filler metal without boron and silicon for brazing of heat-resistant nickel alloy. *Automatic Welding*, 8, 15–21. doi: <https://doi.org/10.15407/as2017.08.02>
29. Myal'nitsa, G. F., Maksuita, I. I., Kvasnitskaya, Yu. G., Mihnyan, E. V. (2013). Selection of new-alloying corrosion-resistant alloy for the nozzle blades. *Metaloznavstvo ta obrobka metaliv*, 2, 29–34. Available at: http://nbuv.gov.ua/UJRN/MOM_2013_2_8
30. Kablov, E. N., Petrushin, N. V., Vasilenok, L. B., Morozova, G. I. (2000). *Reniy v zharoprochnykh nikelvykh splavakh dlya lopatok gazovykh turbin*. *Materialovedenie*, 2, 23–29.

31. Kablov, E. N., Petrushin, N. V., Vasilenok, L. B., Morozova, G. I. (2000). Reniy v zharoprochnykh nikelovykh splavakh dlya lopatok gazovykh turbin (prodolzhenie). *Materialovedenie*, 3, 38–43.
32. Petrunin, I. E., Bereznikov, Yu. I., Bun'kina, R. R., Il'ina, I. I., Markova, I. Yu., Kiselev, I. I. et. al.; Petrunin, I. E. (Ed.) (2003). *Spravochnik po payke*. Moscow: Mashinostroenie, 480.
33. Kvasnitskiy, V. V., Timchenko, V. L., Khorunov, V. F. (1998). Die Untersuchung des Systems Ni(Nileg)-Hf-Zr für das Löten warmfester Nickellegierungen. *DVS-Berichte: Band 192*. Düsseldorf: DVS – Verl, 257–259.
34. Kablov, E. N., Svetlov, I. L., Petrushin, N. V. (1997). Nikelevye zharoprochnye splavy dlya lit'ya lopatok s napravlennoy i monokristallicheskoy strukturoy. *Chast' 1*. *Materialovedenie*, 4.
35. Massalski, P. R., Subramanian, H. O., Okamoto, H., Kacprzak, I. (Eds.) (1990). *Binary Alloy Phase Diagrams*. Vol. 3. Ohio: ASM International Materials Park, 3589.
36. Gayduk, S., Kononov, V. (2016). Phase composition calculation by CALPHAD-method of hightemperature corrosion-resistant weldable nickel-base cast alloy. *Vestnik dvigatelestroeniya*, 1, 107–112. Available at: http://nbuv.gov.ua/UJRN/vidv_2016_1_21
37. Koneva, N. A., Popova, N. A., Kalashnikov, M. P., Nikonenko, E. L., Fedorishcheva, M. V., Pasenova, A. D., Kozlov, E. V. (2013). Vliyanie temperatury deformatsii na fazoviy sostav i strukturu intermetallida Ni3Al, legirovannogo borom i gafniem. *Fundamental'nye problemy sovremennogo materialovedeniya*, 10 (3), 340–348. Available at: <https://core.ac.uk/download/pdf/287457681.pdf>
38. Samsonov, G. V., Vinnitskiy, I. M. (1976). *Tugoplavkie soedineniya*. Moscow: Metallurgiya, 560.
39. Matsugi, K., Murata, Y., Morinaga, M., Yukawa, N. (1992). Realistic Advancement for Nickel-Based Single Crystal Superalloys by the d-Electrons Concept. *Superalloys 1992 (Seventh International Symposium)*. doi: https://doi.org/10.7449/1992/superalloys_1992_307_316